2764–2776 *Nucleic Acids Research, 2008, Vol. 36, No. 8* *Published online 26 March 2008*
doi:10.1093/nar/gkn115

Intracellular delivery of an anionic antisense oligonucleotide via receptor-mediated endocytosis

Md Rowshon Alam[1], Vidula Dixit[1], Hyunmin Kang[1], Zi-Bo Li[2], Xiaoyuan Chen[2], JoAnn Trejo[1], Michael Fisher[1] and Rudy L. Juliano[1,*]

[1]Department of Pharmacology, School of Medicine, University of North Carolina, Chapel Hill NC 27599 and [2]Department of Radiology, Stanford University School of Medicine, Stanford, CA 94305-5484, USA

Received January 14, 2008; Revised February 14, 2008; Accepted February 19, 2008

ABSTRACT

We describe the synthesis and characterization of a 5′ conjugate between a 2′-*O*-Me phosphorothioate antisense oligonucleotide and a bivalent RGD (arginine–glycine–aspartic acid) peptide that is a high-affinity ligand for the αvβ3 integrin. We used αvβ3-positive melanoma cells transfected with a reporter comprised of the firefly luciferase gene interrupted by an abnormally spliced intron. Intranuclear delivery of a specific antisense oligonucleotide (termed 623) corrects splicing and allows luciferase expression in these cells. The RGD–623 conjugate or a cationic lipid-623 complex produced significant increases in luciferase expression, while 'free' 623 did not. However, the kinetics of luciferase expression was distinct; the RGD–623 conjugate produced a gradual increase followed by a gradual decline, while the cationic lipid-623 complex caused a rapid increase followed by a monotonic decline. The subcellular distribution of the oligonucleotide delivered using cationic lipids included both cytoplasmic vesicles and the nucleus, while the RGD–623 conjugate was primarily found in cytoplasmic vesicles that partially co-localized with a marker for caveolae. Both the cellular uptake and the biological effect of the RGD–623 conjugate were blocked by excess RGD peptide. These observations suggest that the bivalent RGD peptide–oligonucleotide conjugate enters cells via a process of receptor-mediated endocytosis mediated by the αvβ3 integrin.

INTRODUCTION

Antisense oligonucleotides, small interfering RNAs (siRNA) and micro RNAs (miRNA) have elicited great interest both as laboratory reagents and as possible therapeutic entities. A number of issues associated with use of oligonucleotides, including potency and stability in the biological milieu, have been addressed through a variety of chemical modifications (1–3). However, in terms of therapeutic use of antisense, siRNA or miRNA oligonucleotides, a key remaining issue is that of effective delivery (4,5). There is abundant evidence that both antisense and siRNA oligonucleotides can exert therapeutic effects in animal models when administered as 'free' compounds, that is, in the absence of any delivery agent (6–8). Moreover, a number of clinical trials of both antisense and siRNA agents as free compounds are underway (9). Nonetheless, many investigators believe that the therapeutic potential of oligonucleotides could be improved by use of appropriate delivery systems.

A variety of approaches have been used to enhance delivery of siRNA and antisense oligonucleotides. In the case of siRNA, viral vector systems are an obvious important possibility (10–12). Various synthetic nanocarriers including liposomes, polymeric nanoparticles and dendrimers have also been extensively studied as oligonucleotide delivery agents (13–17). However, the particulate nature of these materials may limit their biodistribution *in vivo* (18). Thus, in addition to nanoparticle carriers, there is also merit in exploring the use of molecular scale conjugates or complexes of oligonucleotides for delivery purposes. One approach has been to chemically conjugate oligonucleotides with various peptide ligands, including so-called 'cell-penetrating peptides' (CPPs). A number of CPPs have been described; they are most commonly polycationic sequences that seem to have the ability to penetrate from the outside of the cell to the cytosol, and in doing so to assist in delivery of linked 'cargo' molecules, including peptides and proteins (19,20). A considerable effort has gone into the preparation and evaluation of conjugates of CPPs and oligonucleotides; however, on the whole this has been only modestly successful (21,22). While our laboratory has reported some biological effects

*To whom correspondence should be addressed. Tel: 919 966 4383; Fax: 919 966 5640; Email: arjay@med.unc.edu

The authors wish it to be known that, in their opinion, the first two authors should be regarded as joint First Authors

of conjugates of CPPs with anionic antisense oligonucleotides (23,24), and others have reported on CPP–siRNA conjugates (25,26), the prevailing literature suggests that CPPs are only able to effectively deliver oligonucleotides with uncharged backbones, such as peptide nucleic acids and morpholino compounds (27–31). Further, the concentrations needed to elicit biological effects were often in the micromolar range, higher than is usually deemed desirable for potential therapeutic agents.

A potentially more promising strategy is to deliver antisense and siRNA oligonucleotides via receptor-mediated endocytosis by linking the oligonucleotide to a targeting moiety that binds with high affinity to a cell surface receptor capable of undergoing internalization. For example, an aptamer–siRNA conjugate targeting prostate-specific membrane antigen (PSMA) was able to effectively deliver the associated siRNA to prostate cells (32), while a single-chain antibody-protamine chimera, when complexed to siRNA, was able to deliver the siRNA to cells that expressed the target antigen (33). In addition, a peptide that binds the IGF1-receptor was able to deliver a peptide nucleic acid antisense moiety to the cytoplasm of cells expressing the receptor (34).

In this report, we describe the preparation and characterization of conjugates between an anionic antisense oligonucleotide and a bivalent RGD peptide that binds with high affinity to the αvβ3 integrin (35). Members of the integrin family of cell surface receptors provide structural linkages between the extracellular matrix and the cytoskeleton, but are also importantly involved in the control of signal transduction pathways (36). The αvβ3 integrin is of particular interest in cancer since it is highly expressed both in angiogenic endothelial cells and certain types of malignant cells (37). Thus, it may provide a means to selectively target growth-regulatory oligonucleotides to tumors or tumor vasculature. In the current study, the bivalent peptide was coupled to a 'splice-shifting oligonucleotide' (SSO) designed to correct splicing of an aberrant intron inserted into the firefly luciferase reporter gene (38). Thus, successful delivery of the SSO to the cell nucleus would result in up-regulation of luciferase activity. Using this approach we show that the bivalent RGD peptide can effectively deliver the SSO to αvβ3-expressing melanoma cells in culture via a receptor-mediated endocytotic process.

MATERIALS AND METHODS

Synthesis and chemical characterization of peptide-oligonucleotide conjugates

The 2′-*O*-Me phosphorothioate sequence termed oligonucleotide 623 (5′-GTT ATT CTT TAG AAT GGT GC-3′) and its conjugates, as well as mismatched controls, were prepared as described subsequently.

Phosphoramidites, controlled pore glass supports and other reagents. 5′-*O*-(4,4′-Dimethoxytrityl)-*N*-phenoxyacetyl-2′-*O*-methyl-adenosine-3′-*O*-[(β-cyanoethyl)-(*N,N*-diisopropyl)]-phosphoramidite (2′-*O*-Me-Pac-A-CE Phosphoramidite), 5′-*O*-(4,4′-dimethoxytrityl)-*N2*-isopropylphenoxyacetyl-2′-*O*-methyl-guanosine-3′-*O*-[(β-cyanoethyl)-(*N,N*-diisopropyl)]-phosphoramidite (2′-*O*-Me-iPr-Pac-G-CE Phosphoramidite), 5′-*O*-(4,4′-dimethoxytrityl)-*N*-acetyl-cytidine-2′-*O*-methyl-3′-*O*-[(β-cyanoethyl)-(*N,N*-diisopropyl)]-phosphoramidite (2′-OMe-Ac-C-CE Phosphoramidite), 1-*O*-(4,4′-dimethoxytrityl)-hexyl-disulfide-1′-[(β-cyanoethyl)-(*N,N*-diisopropyl)]-phosphoramidite (Thiol-Modifier C6 S-S), 1-*O*-(4,4′-dimethoxytrityl)-3-{*O*-[*N*-carboxy-(tetramethyl-rhodamine)-3-aminopropyl]}-propyl-2-*O*-succinoyl-long chain alkylamino-controlled pore glass (CPG) (3′-Tamra CPG), 3H-1,2-benzodithiole-3-one-1,1-dioxide (Beaucage Reagent) and other reagents for DNA synthesis were purchased from Glen Research (Sterling, VA, USA). 5′-*O*-(4,4′-dimethoxytrityl)-5-methyluridine-2′-*O*-methyl-3′-*O*-[(β-cyanoethyl)-(*N,N*-diisopropyl)]-phosphoramidite (2′-*O*-Me-T-CE Phosphoramidite) was purchased from Chemgenes (Ashland, MA, USA).

Synthesis, cleavage and de-protection of oligonucleotides. Oligonucleotides were synthesized using phosphoramidites of the ultraMILD-protected bases indicated above on a 1 μmol scale on 3′-Tamra CPG supports (500 Å) using a AB 3400 DNA synthesizer (Applied Biosystems, Foster City, CA, USA). The coupling times for the phosphoramidites of ultraMILD-protecting bases and 5′-thiol linker were 360 and 600 s, respectively. 5-Ethylthio-1H-tetrazole was used as an activator (0.25 M solution in acetonitrile), 5% phenoxyacetic anhydride in tetrahydrofuran/pyridine as a CAP mix A, and Beaucage reagent was used to introduce the internucleotide phosphorothioate backbone during oligonucleotide synthesis. A 5′-thiol linker was introduced at the 5′-end of the oligonucleotide.

Oligonucleotides were simultaneously cleaved from the CPG support and deprotected using a mixture of tert-butylamine : methanol : water (1 : 1 : 2) at 55°C for 8 h. Prior to deprotection, the CPG supports were treated with a 10% solution of diethylamine in acetonitrile. This removes cyanoethyl protection and prevents elimination of the 3′-Tamra linker from the oligonucleotide. This was done with disposable syringes using 2 × 1 ml solution for 5 min each followed by washing with acetonitrile and drying the support with a stream of argon gas. The CPG support was then transferred to a vial and 2 ml deprotection solution was added and heated for 8 h at 55°C. The oligonucleotide solution was immediately evaporated to dryness, and resuspended in 0.1 M TEAA buffer for purification.

Purification and structure determination. Purification of the oligonucleotides was carried out by reverse-phase HPLC using a ZORBAX 300 SB-C_{18} column (9.4 mm × 25 cm) on a Varian HPLC system (ProStar/Dynamax, Walnut Creek, CA) with a dual wavelength UV detector. HPLC conditions were as follows: linear gradient, % buffer B = 10–30%/20 min, ~100%/30 min, 4 ml/min; buffer A contained 0.1 M TEAA, pH 7.0 and buffer B: acetonitrile; UV monitor: 254 and 550 nm (λ_{max} for Tamra). The oligos were collected and lyophilized. Structures of the oligonucleotides were determined using

MALDI-TOF (matrix-assisted laser desorption ionization time-of-flight) mass spectroscopy in a positive ion mode on a Voyager Applied Biosystem instrument (Foster City, CA). The matrix used for preparing the oligonucleotide samples was a mixture of 3-hydroxypicolinic acid (50 mg ml^{-1} in 50% aqueous acetonitrile) and diammonium hydrogen citrate (50 mg ml^{-1} in HPLC grade water). The accuracy of the mass measurement was ±0.02%.

Preparation of 5′-thiol oligonucleotides. The 5′-thiol functionality was generated by treating the disulphide bond of the oligonucleotide with 100 mM of aqueous DTT in 0.1 M TEAA buffer containing 1% triethylamine. After overnight incubation, the reaction mixture was desalted through a Sep-PAK® C18 cartridge, and any residual amount of DTT was removed by washing with 5% acetonitrile in a 0.1 M TEAA buffer. Finally, the Tamra-623-SH oligonucleotide was eluted with 50% aqueous acetonitrile and directly used for the conjugation reaction. The structure of the thiol-containing oligonucleotide was confirmed by MALDI-TOF as described above.

Synthesis of bivalent RGD peptide–oligonucleotide conjugates. The synthesis and characterization of similar bivalent RGD peptides has been described elsewhere (35); however, in the present case, a maleimide linker was incorporated so as to allow conjugation with the oligonucleotide. The cyclic RGD dimer (10 μmol) was reacted with maleimide NHS ester (15 μmol) in borate buffer (0.05 N, pH 8.5) at room temperature. After 2 h, RGD–maleimide was isolated by semi-preparative HPLC with a 70% yield. Mass spectrometry analysis [MALDI-TOF-MS: 1515.72 for $[MH]^+$ ($C_{67}H_{95}N_{20}O_{21}$, calcd [MW] 1515.69)] confirmed the product identification. Thiol oligonucleotides (316 nmol in 50% aqueous CH_3CN) were reacted with the maleimide-containing bivalent RGD peptide (475 nmol in water) in a reaction buffer (final salt concentration adjusted to 400 mM KCl, 40% aqueous CH_3CN). The reaction mixture was vortexed and allowed to stand for 3 h, and purified by HPLC using a 1 ml Resource Q column (GE Healthcare, Uppsala, Sweden) following a published method (39). Buffers were as follows: buffer A, 20 mM Tris–HCl (pH 6.8), 50% formamide; buffer B, 20 mM Tris–HCl (pH 6.8), 400 mM $NaClO_4$, 50% formamide; linear gradient, % buffer B = 0–100%/20 min, 3 ml min^{-1}; UV monitor, 254 and 550 nm. The purified conjugates were dialyzed versus milli-Q water, and analyzed by MALDI-TOF using a matrix that was a mixture of 2,6-dihydroxyacetophenon (20 mg ml^{-1}) and diammonium hydrogen citrate (40 mg ml^{-1}) in 50% aqueous methanol. It should be noted that various versions of the bivalent RGD peptide–623 conjugate were made including with or without the Tamra fluorophore, as well as control conjugates having an oligonucleotide with multiple mismatches in the 623 sequence (Table 1).

Table 1. MALDI-TOF mass of oligonucleotides and their RGD conjugates

Oligo/Conjugate	MW_{Calcd}	MW_{Found}
623-Tamra	7691.97	7691.80
HS-$(CH_2)_6$–623-Tamra	7910.74	7912.01
Bivalent-RGD-Mal-S-$(CH_2)_6$–623-Tamra	9427.32	9427.43
5MM623-Tamra	7620.00	7620.20
HS-$(CH_2)_6$–5MM623-Tamra	7833.26	7833.50
Bivalent-RGD-Mal-S-$(CH_2)_6$–5MM623-Tamra	9347.95	9345.50

623 sequence: 5′-GTT ATT CTT TAG AAT GGT GC; 5MM623 sequence: 5′-GTA ATT ATT TAT AAT CGT CC.

Cell lines and plasmids

A375SM melanoma cells were obtained from Dr J. Bear (University of North Carolina), and were cultured in Dulbecco's minimum essential medium (DMEM) (Gibco/Invitrogen, Carlsbad, CA, USA) supplemented with L-glutamine and 10% fetal bovine serum (FBS). M21+ and M21− melanoma cell lines, having or lacking αvβ3 integrin expression (40) were obtained from Dr D. Cheresh (University of California, San Diego) and were similarly maintained. Plasmid pLuc/705, containing an aberrant intron inserted into the firefly luciferase coding sequence, was a kind gift from Dr R. Kole, (University of North Carolina) (38). Stable transfectants were obtained by co-transfecting A375SM cells with one part of hygromycin-resistant plasmid pcDNA3.1(+)/hygro (Invitrogen) and 10 parts of pLuc/705 using Lipofectamine 2000 as per manufacturer's instructions. Selection was carried out in DMEM containing 200 μg/ml hygromycin and 10% FBS. The resulting pool of hygromycin-resistant cells was referred to as A375SM-Luc705-B.

Oligonucleotide treatment and luciferase assay

A375SM-Luc705-B cells were plated on 12-well plates (at 1.0 or 1.5×10^5 cells per well in various experiments) in DMEM supplemented with 10% FBS. The following day, medium was changed to reduced serum OPTI-MEM I (Gibco, Carlsbad, CA, USA). Cells were treated with either free 623 oligonucleotide, 623 complexed with Lipofectamine 2000® as per manufacturer's instruction, or RGD–623 conjugate or with mismatched control oligonucleotides. Four hours after treatment, 1% FBS was added to each well. Twenty-four hours after oligonucleotide treatment, medium was replaced with DMEM containing 1% FBS, and at various times thereafter cell lysates were collected for luciferase assay. Cells were usually harvested 48 h after oligonucleotide treatment, or at times indicated in the figures, and activity determined using a Luciferase assay kit (Promega, Madison, WI, USA). Measurements were performed on a Monolight 2010 instrument (Analytical Luminescence Laboratory, San Diego, CA, USA). In some cases, the effects of the RGD–623 conjugate were evaluated in the presence of free monovalent cyclic RGDfV peptide (Anaspec, San Jose, CA, USA).

Cell uptake, confocal fluorescence microscopy and flow cytometry

Total cellular uptake of Tamra-labeled oligonucleotides was monitored using a Nanodrop microfluorimeter (Nanodrop Technologies, Wilmington, DE, USA). After treatment with oligonucleotides the cells were lysed in a mild non-ionic detergent buffer and the Tamra

fluorescence (emission 583 nm) was quantitated based on a linear standard curve of unconjugated Tamra in buffer.

Intracellular distribution of Tamra-labeled oligonucleotides in living cells was examined using an Olympus Confocal FV300 fluorescent microscope with 60X-oil immersion objective, as previously described (41). Co-localization of Tamra-labeled oligonucleotides with Alexa-488 labeled transferrin or 10 000 MW dextran (Molecular Probes, Beaverton, OR, USA), as markers for clathrin-coated vesicles or smooth vesicles, respectively (42), was also done by confocal microscopy. Sub-cellular localization of Tamra-labeled oligonucleotides in specific endomembrane compartments was monitored by fixing cells with 4% paraformaldehyde followed by permeabilization with methanol for 30 s (43) and treatment with primary antibody followed by Alexa488-labeled secondary antibody. Antibodies to the following endomembrane markers (40,44,45) were obtained from BD Biosciences (San Jose, CA): caveolin-1 (caveolae), EAA1 (early endosomes), p230TG (trans-Golgi), LAMP1 (lysosomes), clathrin (coated vesicles). Primary and secondary antibodies were used at a 1 : 1000 dilution. Visualization of markers by confocal fluorescence microscopy followed previously described approaches (46,47). Expression levels of αvβ3 were monitored by immunostaining with an anti-human-αvβ3 monoclonal (Chemicon, Temecula, CA, USA) followed by an Alexa 488 rabbit anti-mouse secondary antibody, with analysis by flow cytometry using a DakoCytomation (Glostrop, Denmark) machine. Cytochalasin D and β-cyclodextrin were purchased from Sigma Chemical Co.

Toxicity studies

For short-term studies, cells were treated with various concentrations of oligonucleotides or conjugates under the same conditions as used for the luciferase-induction experiments. After 48 h in medium plus 1% FBS, cells were trypsinized and viable cells were counted in a Cellzone® electronic particle counter (Elmhurst, IL). Long-term toxicity was assessed using a colony-formation assay. Thus, cells were treated with various concentrations of oligonucleotides or conjugates under the same conditions as used for the luciferase induction experiments. Thereafter, cells from each treatment group were replated in 6-well plates containing a mixture 1% low gelling temperature agarose (SeaKem, Rockland, ME, USA) and complete DMEM-H medium with 10% FBS. After 14 days, surviving colonies larger than 25 cells were counted. Survival was expressed as colonies per 100 cells plated.

RESULTS

Oligonucleotide 623 is a 2′-*O*-Me phosphorothioate sequence that is designed to correct splicing of an aberrant intron from thalassemic hemoglobin; this intron can be inserted into various reporter genes, such as luciferase, and correction of the splicing defect results in up-regulation of gene expression (48,49). This provides a sensitive and convenient positive readout for monitoring delivery of splice switching oligonucleotides (SSOs) to the cell nucleus, the compartment where splicing takes place. It also avoids the typical pitfalls of many assays of antisense or siRNA effects that rely on inhibition of gene expression and can thus be confounded by non-specific toxicities. In the current report, we have linked the 623 SSO to a peptide that contains two modules of a cyclic RGD sequence. This allows the bivalent peptide to bind with high affinity to the αvβ3 integrin (35), a cell surface receptor that is highly expressed in angiogenic endothelial cells and certain types of tumor cells, including the A375 melanoma cells used here.

Synthesis and characterization

The chemical structure of the bicyclic RGD peptide is shown in Figure 1A. This peptide contains a maleimide functionality that can be coupled with 5′-thiol oligonucleotide 623 via the Michael addition reaction as shown in Figure 1B. We introduced a Tamra fluorophore at the 3′-end of the oligonucleotide and a thiol C-6 S-S linker at the 5′-end. The DMTr-$(CH_2)_6$-S-S-$(CH_2)_6$-[623]-Tamra oligonucleotide (**1**) was purified by RP-HPLC, and its disulfide bridges were reduced with DTT solution to generate highly reactive 5′-HS-$(CH_2)_6$-[623]-Tamra oligonucleotide (**2**).

The peptide conjugation reaction occurred between the maleimide of the bicyclic RGD peptide and the 5′ thiol (-SH) of the oligonucleotide (**2**). The reaction proceeded efficiently and >95% of the starting oligonucleotide (**2**) was converted into conjugates with bicyclic RGD. The conjugates were purified by ion-exchange chromatography (Resource Q column) under highly denaturing conditions (39) to avoid any sort of precipitation, although this was not expected to be a problem for this type of peptide. HPLC profiles for the purified bicyclic RGD–623 conjugate and for the thiol oligonucleotide (**2**) are given in Figure 1C, which shows that the conjugate peak is clearly resolved from the starting thiol oligonucleotide. After dialysis and lyophilization, the conjugate re-dissolved in sterile water without any difficulty. Similar approaches were used for the preparation of other oligonucleotides and conjugates. In each case, the structure of the final product was confirmed by MALDI-TOF mass spectroscopy. The characteristics of the various oligonucleotides and conjugates synthesized are given in Table 1.

Dose–response studies

The RGD–623 conjugate, as well as 'free' 623, or 623 complexed with Lipofectamine 2000 were incubated with A375SM-Luc705-B cells as described in Materials and methods section and the cells were tested for luciferase expression. As seen in Figure 2A, the RGD–623 conjugate produced a significant increase in luciferase expression while the free 623 did not. The effect of higher concentrations of RGD–623 was ~50% of that produced by the 623/cationic lipid complex. It should be noted that we were not able to use >100 nM oligonucleotide with the Lipofectamine 2000 complexes because this material became quite toxic at higher concentrations of oligonucleotide. Although we have not performed a highly detailed dose–response study, our current data suggests

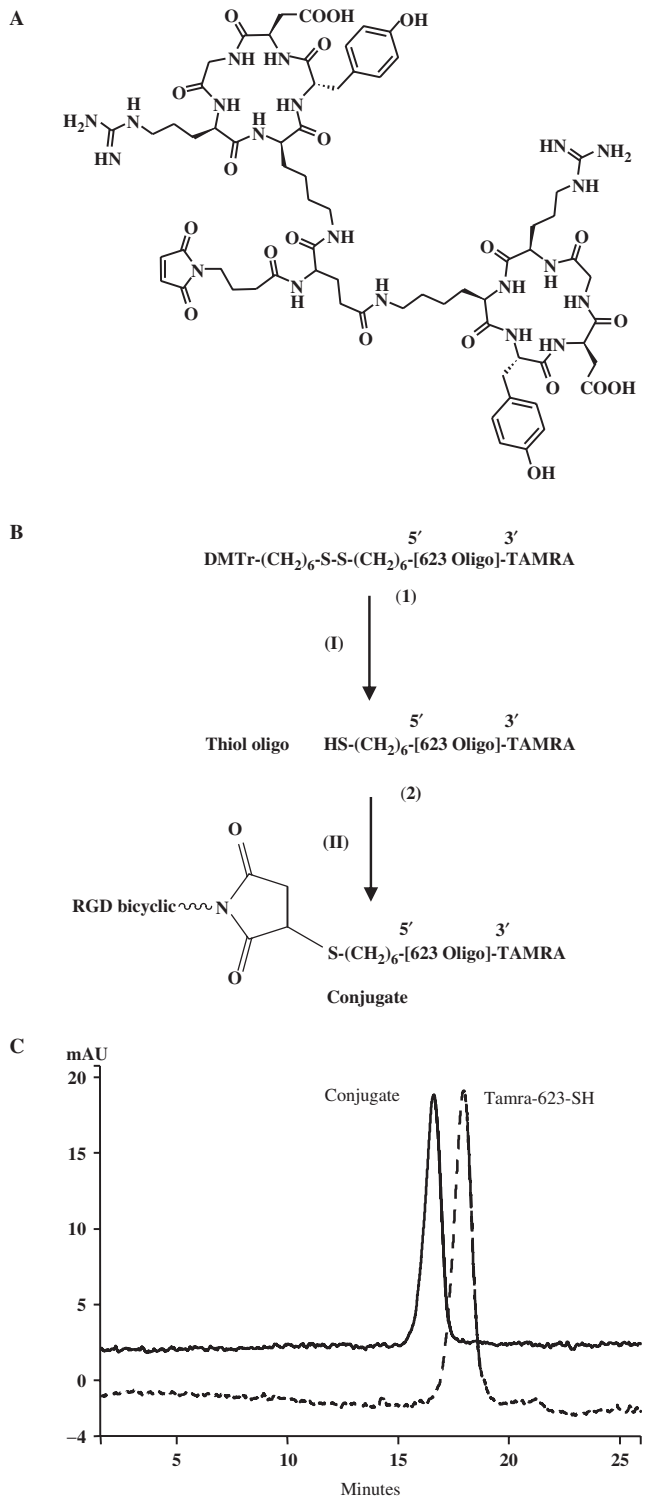

Figure 1. (**A**) Chemical structure of the maleimide-bicyclic RGD peptide. The maleimide reactive group is positioned mid-way along a linker that joins the two cyclic RGD moieties. (**B**) Synthetic scheme for the conjugation of oligonucleotide 623 to the bivalent RGD peptide. The intermediates (1, 2) were purified after each step in the synthesis. (I) 100 mM DTT, 0.1 M TEAA buffer, 1% triethylamine; (II) maleimide-bicyclic-RGD peptide in H_2O (1.5 equivalent), 400 mM KCl, 40% CH_3CN, 3 h, RT. (**C**) HPLC analysis of the RGD peptide–oligonucleotide conjugate. HPLC analysis was performed as described in Materials and methods section. The elution profiles of the 5′-SH-3′-Tamra 623 oligonucleotide and its bivalent RGD conjugate are shown.

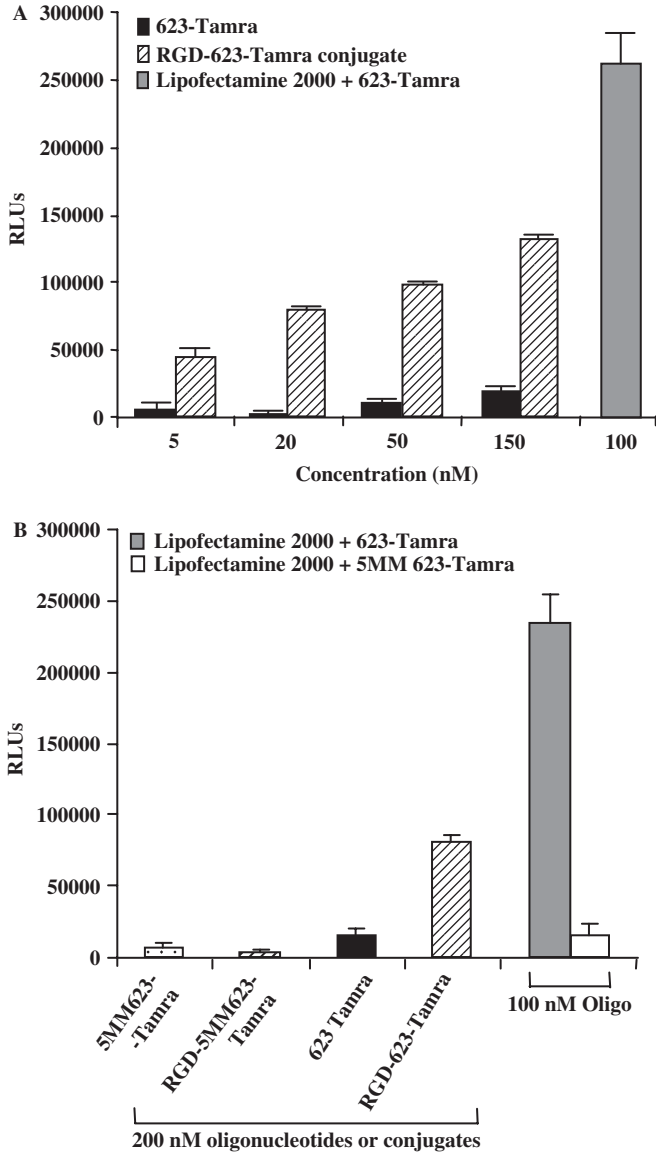

Figure 2. Dose–response and specificity studies. (**A**) Cells were treated with either 623-Tamra, RGD–623-Tamra conjugate or 623-Tamra complexed with Lipofectamine 2000, as described in Materials and methods section, and luciferase activity was determined after 48 h and expressed as relative luminescence units (RLUs) per 1.5×10^5 cells. Black bars represent luciferase activity of 623-Tamra, patterned/striped bars represent the RGD–623-Tamra conjugate and the gray bar represents the activity of 100 nM 623-Tamra transfected using Lipofectamine 2000. (**B**) The effect of 623-Tamra or RGD–623-Tamra was compared to controls having five mismatched bases (indicated as 5MM623). The conjugates or free oligonucleotide were used at 200 nM while the Lipofectamine 2000 complexes were used at 100 nM oligonucleotide. Results (A and B) are the means and standard errors of three determinations.

that the effect of the RGD–623 conjugate rises steadily between 0 and 100 nM and then begins to plateau. This behavior is consistent with the known affinities of the bivalent RGD peptide and its conjugates for the αvβ3 integrin, these being approximately in the 15–30 nM range (35). Use of a control oligonucleotide or a control RGD-conjugate, each having five mismatches in the 623 sequence, failed to produce an increase in luciferase

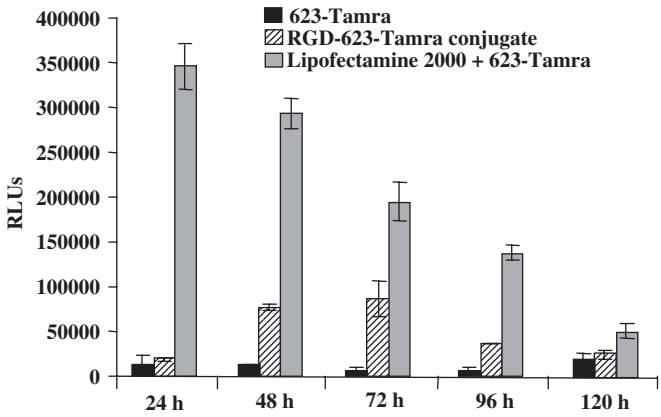

Figure 3. Time–response studies. Cells were treated with either 623-Tamra, RGD–623-Tamra conjugate or 623-Tamra complexed with Lipofectamine 2000, as described in Materials and methods section, and luciferase activity was determined at the times indicated. Black bars represent luciferase activity of 200 nM 623-Tamra, patterned/striped bars represent 200 nM RGD–623-Tamra conjugate and gray bars represent 100 nM 623-Tamra transfected using Lipofectamine 2000, all expressed as RLUs per 10^5 cells. Results are the means and standard errors of triplicate determinations.

expression (Figure 2B), indicating that the luciferase response observed depends on specific base-pairing. We also examined whether the presence of the Tamra fluorophore affected the action of the 623 oligonucleotide on luciferase expression. We found that neither the effects of RGD–623 nor of 'free' 623 delivered via lipofection were altered by the inclusion of Tamra at the 3′ position, at concentrations up to 75 nM; at concentrations >100 nM there was a slight augmentation of effect by Tamra presumably due to some hydrophobic binding of the conjugate to the cell membrane (Supplementary Data).

Time–response studies

We examined the kinetics and duration of action of the RGD–623 conjugate by harvesting the cells at various times after the period of exposure to the oligonucleotide. As seen in Figure 3, there was a striking difference between the kinetics of the RGD–623 conjugate and the cationic lipid/623 complex. Thus, the effect of the RGD–623 conjugate on luciferase expression rose gradually with time and reached a maximum at 72 h (48 h after removal of the oligonucleotide). In contrast, the effect of the cationic lipid/623 complex was greatest at very early time points after exposure to the oligonucleotide and declined steadily thereafter. This indicates that the two modes of delivery operate by very different mechanisms. The oligonucleotide delivered via cationic lipids seems to rapidly go to the nucleus, while that delivered via the peptide-conjugate seems to traffic through other intracellular compartments and only gradually reach the nucleus where the effect on splicing takes place.

Total cellular uptake

We evaluated total cellular uptake of 623-Tamra or its RGD-conjugate by incubating cells with various concentrations of these molecules and then measuring total cell-associated fluorescence as described in Materials and methods section. As seen in Figure 4A, there was approximately 2-fold greater uptake of the RGD-conjugate as compared to the unconjugated oligonucleotide at each concentration tested. The increased uptake could largely be blocked by co-incubation with excess free cyclic RGD peptide suggesting the involvement of the αvβ3 integrin (data not shown). As another means of clearly implicating αvβ3 in cellular accumulation of the conjugate, we measured uptake of 623-Tamra or RGD–623-Tamra by M21+ and M21− melanoma cells that have or lack expression of the αvβ3 integrin (Supplementary Data). As indicated in Figure 4B, there was substantially more (~3×) uptake of the RGD-conjugate by the M21+ cells as compared to the M21− cells. In the M21− cells, there was slightly greater uptake of the RGD–623-Tamra conjugate as compared to the 623-Tamra control. However, this might be due to the presence of other RGD-binding integrins such as α5β1 or αvβ1 that could associate with the conjugate, albeit with lower affinity.

To determine whether incubation with RGD–623-Tamra 'down-regulates' expression of its integrin receptor, we examined cell surface levels of αvβ3 before and after 24 h exposure to the RGD conjugate. As seen in Figure 4C, exposure of the cells to 200 nM of RGD–623-Tamra, or 623-Tamra, had no effect on the level of cell surface αvβ3 expression. Thus, the data of Figure 4 indicate that a significant portion of the uptake of the RGD–oligonucleotide conjugate occurs via the αvβ3 integrin, but that this does not result in substantial net loss of αvβ3 from the cell surface, presumably due to efficient recycling of the receptor.

Inhibition of function with excess RGD peptide

We further tested the hypothesis that the RGD–623 conjugates that are functional in affecting luciferase splicing enter the cell via receptor-mediated endocytosis involving the αvβ3 integrin. If that were the case, then the biological effect of RGD–623 should be blocked by co-incubation with excess amounts of a ligand that binds to the same site on αvβ3. As a blocking agent we utilized a cyclic RGD peptide (RGDfV) that is known to be a selective inhibitor of αvβ3 (50,51). Co-incubation with increasing concentrations of this peptide led to a progressive inhibition of the effect of RGD–623-Tamra on luciferase expression (Figure 5). This observation supports the concept that the effect of RGD–623-Tamra on splicing largely depends on its initial uptake via the αvβ3 receptor.

Subcellular distribution

We examined subcellular distribution of the Tamra-labeled oligonucleotides in living cells by confocal fluorescence microscopy (Figure 6A). In the case of cells treated with 623-Tamra complexed with Lipofectamine 2000, a substantial amount of cell uptake was seen; this was primarily associated with cytoplasmic vesicles, while a fraction of the cells clearly had fluorescence within the cell nucleus. With the RGD–623-Tamra conjugate substantial cellular uptake was observed; this was primarily associated with cytoplasmic vesicles and there was no readily

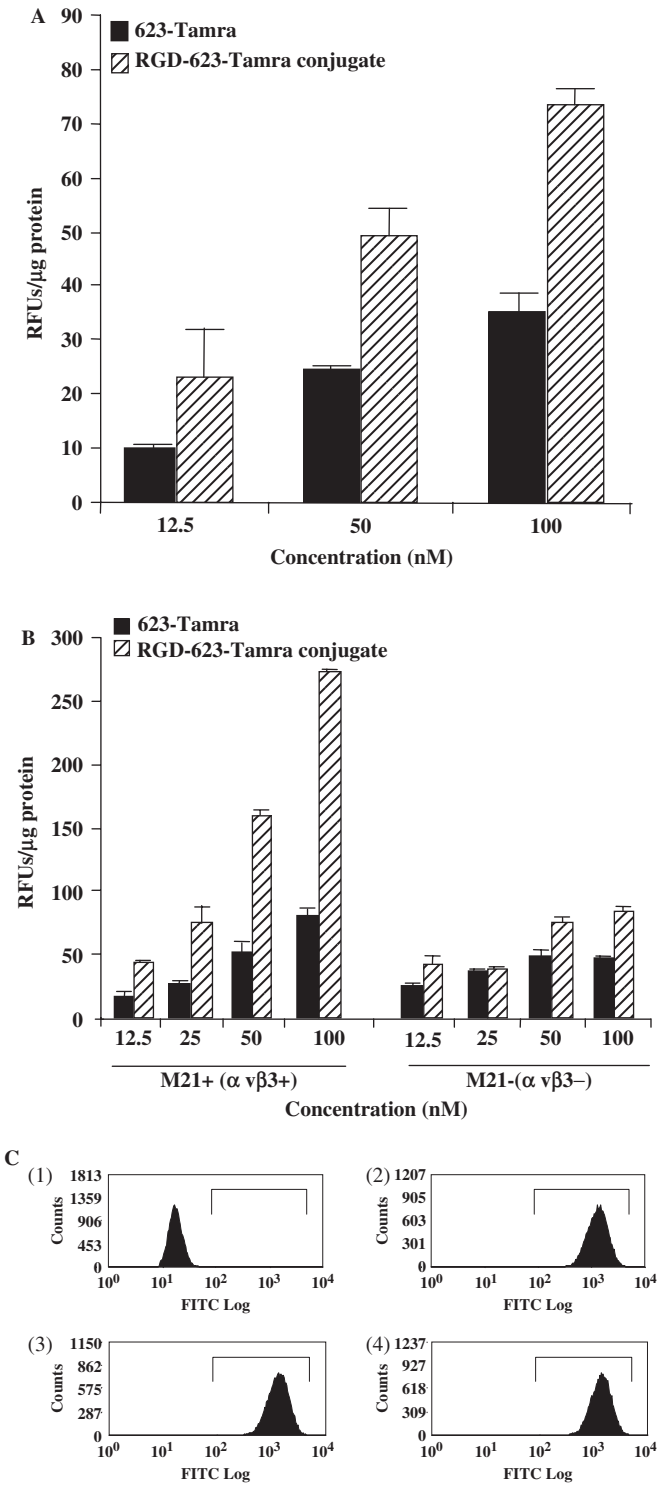

Figure 4. (**A**) Total cell uptake. Cells in 12-well plates were treated with various concentrations of free 623-Tamra, or RGD–623-Tamra, for 4 h in OptiMEM at 37°C, then 1% FBS was added to each well. After 24 h of further treatment, the cells were rinsed three times in buffered saline solution and then lysed. Total cell-associated Tamra was measured using a Nanodrop® fluorimeter as described in Materials and methods section. Results represent means and standard errors of triplicate determinations and are expressed as relative fluorescence units (RFUs) per microgram cell protein. (**B**) Uptake of RGD–623-Tamra depends on αvβ3. Both αvβ3-positive M21+ and αvβ3-negative M21− human melanoma cells were exposed to several concentrations of RGD–623-Tamra or 623-Tamra. Total cell-associated Tamra was measured using a Nanodrop® fluorimeter as described in Materials and methods section. Results represent means and standard errors of triplicate determinations and are expressed as RFUs per microgram cell protein. (**C**) Lack of down-regulation of αvβ3 by RGD–623. A375SM-Luc705-B cells were maintained as controls or were treated with 200 nM RGD–623-Tamra or 623-Tamra for 24 h; thereafter, αvβ3 levels were determined by immunostaining with anti- αvβ3 and flow cytometry as described in Materials and methods section. (1) Cells not stained with primary anti- αvβ3; (2) control cells stained with anti- αvβ3, (3) cells treated with 200 nM RGD–623-Tamra and stained with anti- αvβ3, (4) cells treated with 200 nM 623-Tamra and stained with anti- αvβ3. Ordinate, number of cells; abcissa, log fluorescence intensity.

observable nuclear fluorescence. In the case of 'free' 623-Tamra, less uptake was observed, consistent with the findings in Figure 4A. Co-incubation of the RGD–623-Tamra conjugate with free RGD peptide substantially reduced total cell-associated fluorescence in the confocal images (data not shown).

We undertook a preliminary investigation of the subcellular trafficking of the RGD-conjugate, keeping in mind that endosomal trafficking processes are extremely complex (42,52). Using live cells, we examined the colocalization of the RGD–623-Tamra conjugate with transferrin or dextran, well-known markers, respectively for clathrin-coated vesicle or smooth vesicle endocytosis. At early time points (2 h) there was no co-localization of the RGD-conjugate with transferrin but there was extensive co-localization with dextran (Figure 6B). At later times (24 h) there was substantial co-localization of the RGD-conjugate with either the transferrin or dextran markers. These observations suggest the RGD–oligonucleotide conjugate initially enters cells via a non-clathrin-mediated endocytic process, but eventually trafficks through various endomembrane compartments including some that can also be accessed by transferrin.

To further pursue the subcellular fate of the RGD-conjugate we examined its distribution as compared to well-known markers for several endomembrane compartments, using immuno-localization in fixed and permeabilized cells. It should be noted that we carefully examined the fluorescence patterns of the RGD–623-Tamra conjugate in live and fixed/permeabilized cells and did not observe any significant differences, thus indicating that the conjugate does not re-localize upon fixation and permeabilization. As shown in Figure 7A, at early times (2–6 h) there was significant co-localization of RGD–623-Tamra with caveolin-1. Long 'strands' of caveolin-1-positive endosomes were observed near cell edges, as is sometimes seen for this marker, and some of these apparently contained RGD–623-Tamra. We also noted early (2–6 h) co-localization of RGD–623-Tamra with αvβ3, as one might expect (Figure 7B). Finally, at late (24 h) but not early (6 h or less) times, we observed some co-localization of RGD–623-Tamra with TG230, a marker for the trans-Golgi compartment (Figure 7C). We did not observe significant co-localization of RGD–623-Tamra with other markers tested including EAA1, LAMP1 and clathrin; the last being consistent with our live cell observations (Figure 6B) that the conjugates do not use a clathrin-coated vesicle pathway. While there are always concerns

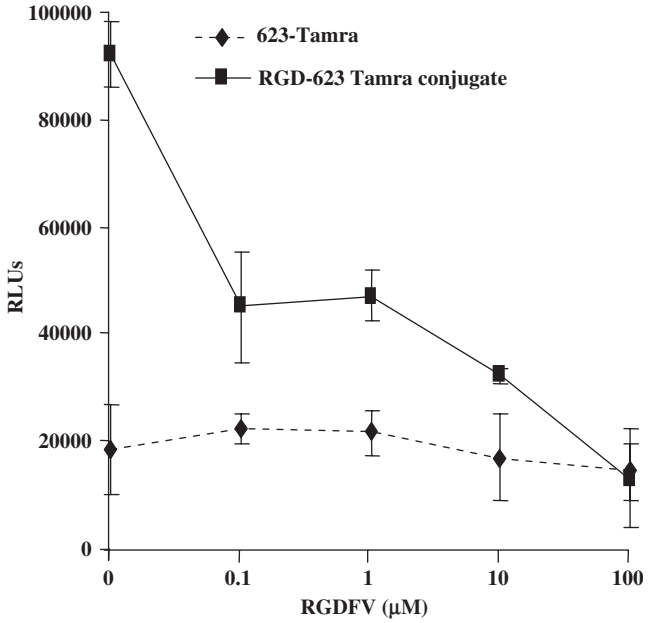

Figure 5. Inhibition of effect with excess RGD peptide. Free RGDfV peptide at the indicated concentrations was added to the cells 30 min prior to treatment with either 623-Tamra or RGD-623-Tamra conjugate, as described in Materials and methods section. Luciferase activity was determined after 48 h. The dotted line represents luciferase activity of 200 nM 623-Tamra, and the solid line represents 200 nM RGD–623-Tamra conjugate. Results are the means and standard errors of triplicate determinations.

about relying on fluorophore labels, the fact that we are using rather stable 2′-O-Me phosphorothiate compounds makes it likely that the 3′-Tamra label provides a reasonably good initial indication of the subcellular distribution of the oligonucleotide. Similar fluorophore-labeled antisense or siRNA oligonucleotides have been widely used to trace subcellular distributions for periods up to 24 h (39,53).

We also examined the effects of some known inhibitors of endocytosis on the ability of cells to accumulate RGD–623-Tamra. As seen in Figure 7D, both β-cyclodextrin and cytochalasin D blocked the uptake of the conjugate. At the non-cytotoxic concentrations used here, β-cyclodextrin is thought to interfere with endocytosis mediated by lipid raft-rich structures, including caveolae, via depletion of cholesterol (54), while cytochalasin D blocks actin filament function (55), which is necessary for virtually all forms of endocytosis (52). While use of pharmacological inhibitors needs to be interpreted cautiously because of possible side-effects, these results do support the fluorescence microscopy observations and suggest that the RGD–oligonucleotide conjugate enters cells via caveolae and possibly other lipid raft-rich smooth endocytotic vesicles.

Toxicity

We have evaluated the short-term toxicity of the oligonucleotides and conjugates used in these studies. As seen in Figure 8, there was little effect of either the 623-Tamra oligonucleotide or its RGD-conjugate at concentrations up to 1000 nM. Some cell rounding was observed at the higher concentrations of RGD–oligonucleotide conjugate, but this did not result in significant cell loss. Although high concentrations of the RGD-conjugate might be expected to perturb adhesion mediated by RGD-binding integrins, in the experimental setting the cells have the opportunity to lay down extracellular matrix and may be anchored to that matrix by both RGD-binding and non-RGD-binding integrins, for example, those involved in binding to collagen or laminin (36). Some toxicity was observed for the Lipofectamine 2000/623-Tamra complex at 100 nM oligonucleotide, while use of 200 nM was very toxic (data not shown). The increased toxicity of the cationic lipid complexes may be due in part to the fact that they are very effective in delivering oligonucleotides to the cell. We also evaluated long-term toxicity using a colony-formation assay. As seen in Table 2 there was little effect of RGD–623-Tamra on the long-term growth abilities of the cells when treated with doses up to 1000 nM. Thus the RGD–oligonucleotide conjugates seem to be well-tolerated by cells over and above the concentration range needed to obtain significant effects in terms of splice correction of the luciferase reporter gene.

DISCUSSION

In this report, we have examined the ability of a bivalent RGD peptide to deliver an antisense oligonucleotide to cells via targeting a specific cell surface receptor, the αvβ3 integrin. The 2′-*O*-Me phosphorothioate oligonucleotide used here (oligonucleotide 623) was designed to correct the splicing of an aberrant intron inserted into the luciferase reporter gene. Thus successful delivery of the 623 oligonucleotide to the nucleus is reflected by an up-regulation of luciferase expression. Dose–response studies monitoring luciferase induction indicated that the RGD–623 conjugate displayed progressively increasing activity in the 5–100 nM range but that activity plateaued at higher concentrations; this may be due to saturation of the αvβ3 receptor by the conjugate. The fact that biological effects are attained in the nanomolar range differentiates the RGD–623 conjugate from other peptide–oligonucleotide conjugates employing various cell-penetrating peptides, since in those cases micromolar concentrations were usually required (21,22). The maximum effects produced by the RGD–623 conjugates ranged from 30% to 60% of that produced by delivering the 623 sequence with Lipofectamine 2000. However, the toxicities associated with cationic lipids make them questionable candidates for *in vivo* delivery (56), while RGD peptide-conjugates are relatively non-toxic even at concentrations well above those needed to elicit a pharmacological effect, and may thus have some potential for *in vivo* applications. The kinetics of the luciferase expression produced by the RGD–623 conjugate entailed a gradual rise and subsequent decline; this would be consistent with initial entry into an endosomal compartment followed by gradual release. In contrast, delivery mediated by cationic lipids results in an initial burst of

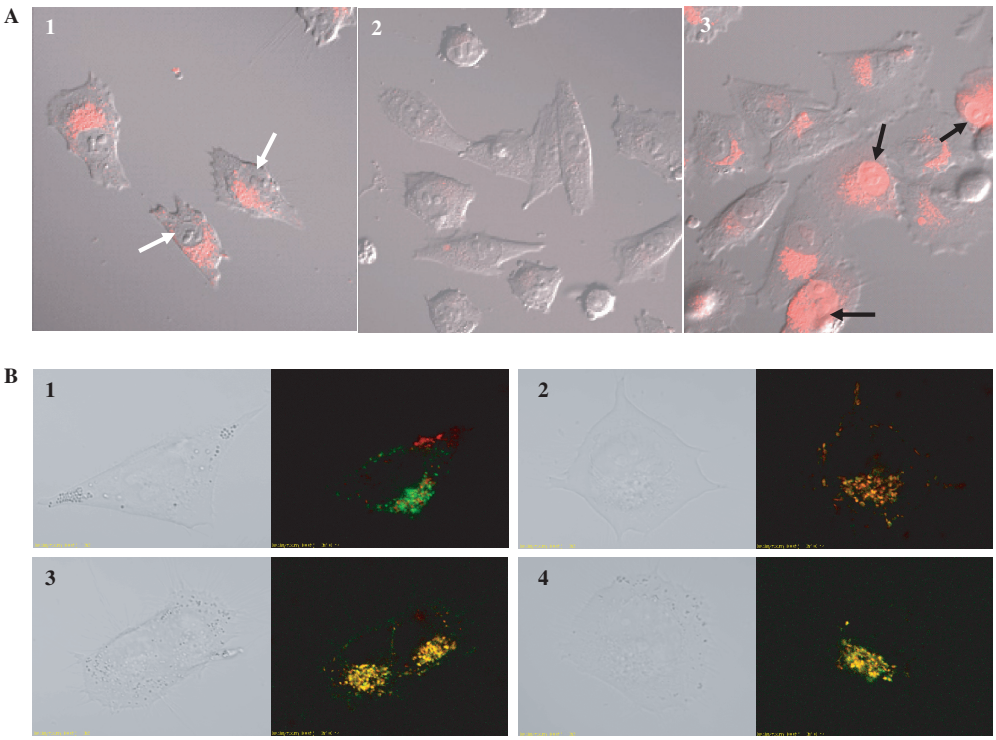

Figure 6. (**A**) Subcellular distribution of the conjugate. A375SM-Luc705-B cells were treated with either 623-Tamra, RGD–623-Tamra conjugate (both 200 nM) or with 623-Tamra complexed with Lipofectamine 2000 (100 nM), as described in Materials and methods section. Cells were observed using confocal fluorescence microscopy. Care was taken to make sure images were acquired from optical sections within the cell. Panel (1) RGD–623-Tamra conjugate, Panel (2) 623-Tamra, Panel (3) 623-Tamra complexed with Lipofectamine 2000. Images shown are overlaps of the Tamra-fluorescence and phase contrast images and are typical of multiple observations. In (1) white arrows indicate the position of the nucleus, while in (3) black arrows indicate nuclei that have accumulated Tamra-oligonucleotide. (**B**) Co-localization with endosomal pathway markers. RGD–623-Tamra oligonucleotide conjugate (100 nM) was co-incubated with: (1) Transferrin–Alexa 488 (200 nM) for 2 h: (2) Transferrin–Alexa 488 (200 nM) for 24 h; (3) Dextran–Alexa 488 (2 μM) for 2 h; (4) Dextran–Alexa 488 (2 μM) for 24 h. Live cells were observed by differential interference contrast (DIC) and confocal fluorescence microscopy as described in Materials and methods section. Concentrations of Alexa 488 transferrin and dextran were chosen to provide brightness similar to the Tamra conjugate. Panel (1) shows no overlap of RGD–623-Tamra (red) and Transferrin–Alexa 488 (green) at 2 h. Panel (3) shows substantial overlap (yellow-orange) of RGD–623-Tamra and Dextran–Alexa 488 at 2 h. Panels (2) and (4) show substantial overlap of RGD–623-Tamra with both Alexa 488 markers (yellow-orange areas) after 24 h.

luciferase activity followed by a steady decline. Thus the trafficking and delivery mechanisms involved in the two situations are quite distinct. Both cell uptake and biological effects of the RGD–623 conjugate were blocked by co-incubation with excess of a monovalent cyclic RGD peptide that is a specific ligand for the αvβ3 integrin. Additionally, cell uptake of the conjugate was higher in an αvβ3-positive melanoma sub-line than in its αvβ3-negative version. These results strongly suggest that the uptake and delivery process involves receptor-mediated endocytosis of the peptide conjugate.

Using conventional confocal fluorescence microscopy we have observed that the RGD–623-Tamra conjugate is taken up to a greater degree than the unconjugated 'free' 623 oligonucleotide, and that fluorophore-labeled RGD-conjugates accumulate primarily in cytoplasmic vesicles, with little evidence of nuclear accumulation. However, a small but functionally significant fraction of the conjugate must reach the nucleus, since substantial up-regulation of luciferase activity is observed, and RNA splicing only takes place within the nuclear compartment (57). Recent studies of conjugates between CPPs and PNA oligonucleotides have also found that effects on splicing can be attained under circumstances where little or no nuclear localization is observable by fluorescence microscopy (28).

In these studies, we have made use of a relatively stable maleimide coupling to join the RGD-peptide and the oligonucleotide, and have not explored the impact of linker stability on biological outcomes. In previous studies, both bioreversible S–S linkages and more stable linkages have been used successfully with peptide–oligonucleotide conjugates (21,22).

There have been previous reports of RGD-conjugated oligonucleotides (58) as well as reports of a variety of strategies for peptide–oligonucleotide conjugation (59–61). However, the present report differs from earlier studies in two ways. First, we are making use of a dimeric RGD moiety that has a substantially higher affinity than previous RGD ligands. Second, we have undertaken more extensive biological characterization of the RGD–oligonucleotide conjugates than was the case in previous studies. In other contexts, RGD ligands have been widely used to target a variety of drugs, imaging agents, macromolecules and nanocarriers. Thus, there is an extensive literature on the use of mono- and multi-valent

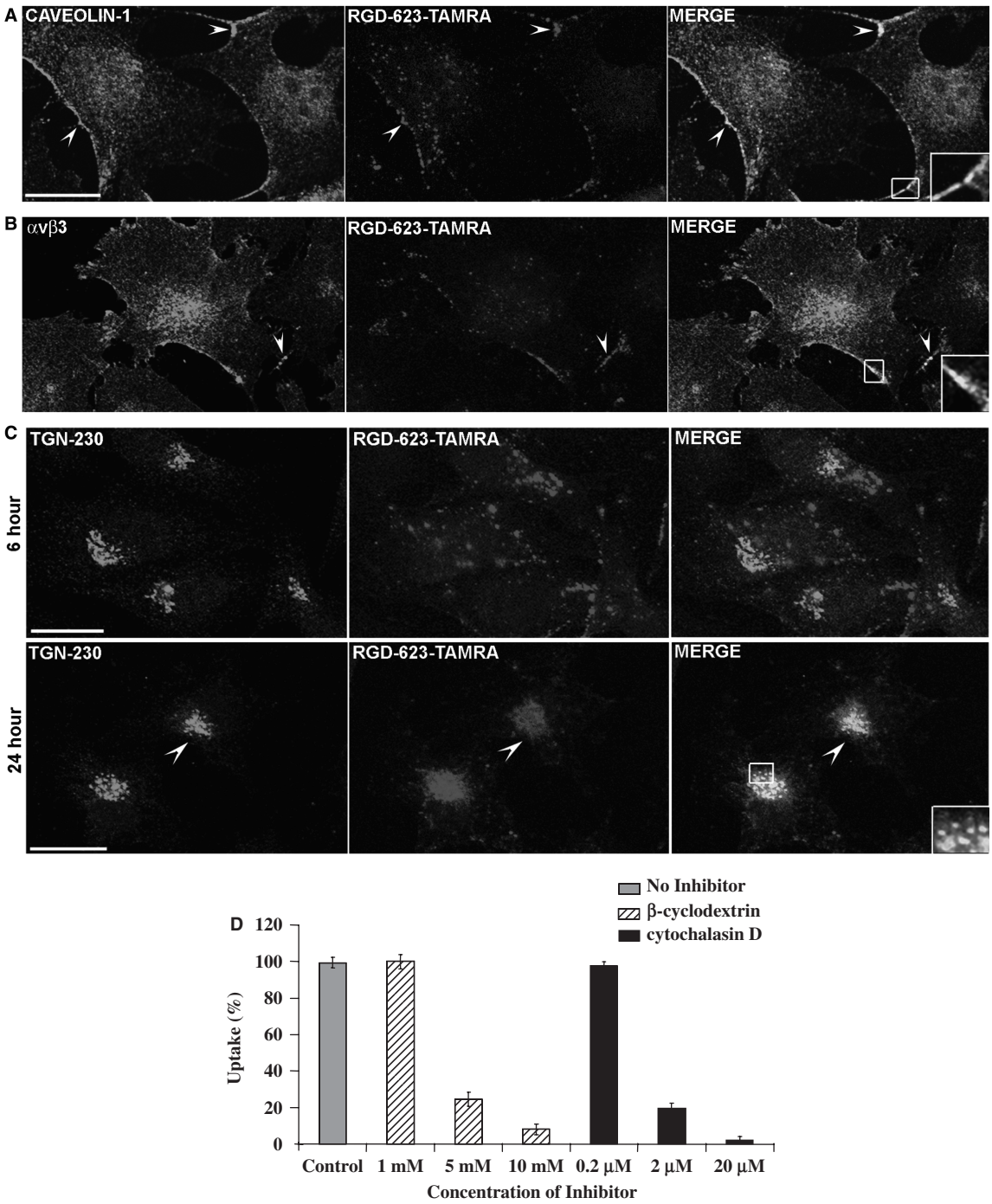

Figure 7. Co-localization with markers of endomembrane compartments and effects of inhibitors. Cells were treated with 50 nM RGD–623-Tamra for various periods and were then fixed, permeabilized and stained with antibodies to markers of various sub-cellular compartments, followed by Alexa 488 secondary antibody, as described in Materials and methods section. Fletches and boxes indicate areas of co-localization; boxed areas are expanded at higher magnification. (**A**) Co-localization with caveolin-1 at 6 h. (**B**) Co-localization with αvβ3 at 6 h. Note that similar patterns were observed during the period 2–6 h. (**C**) Co-localization with a trans-Golgi marker (TGN 230) at 6 or 24 h. (**D**) Cells were treated with cytochalasin D or β-cyclodextrin at the indicated concentrations for 15 min and then 100 nM RGD–623-Tamra was added. Total cell uptake after 4 h was measured using a Nanodrop® fluorimeter as described in Materials and methods section. No loss of cell viability was detected at the concentrations used, although the highest concentration of cytochalasin D caused some cell rounding. Results represent means and standard errors of triplicate determinations and are normalized based on cells receiving no inhibitor as 100%.

RGD peptides linked to PET, SPECT, MRI and fluorescence imaging agents for non-invasive visualization of the distribution of αvβ3 integrin in tumors and in angiogenic vasculature (62–64). RGD ligands have also been linked directly to drugs (35) or, in polyvalent form, to drug–albumin conjugates (65). Various nanocarriers including polymers and Q-dots have also been targeted to cells using RGD ligands (66). These multiple studies attest to the value of high-affinity RGD ligands as a means to attain receptor-selective targeting. There has also been a good deal of interest in use of other receptor-selective ligands for targeted delivery of oligonucleotides, primarily in the context of nanocarriers (67). For example, transferrin has been used to promote selective uptake of cationic nanocarrier–siRNA complexes by tumors (13), while folate has been used to target polyethyleneimine–siRNA (PEI–siRNA) complexes to cells overexpressing the folate receptor (68).

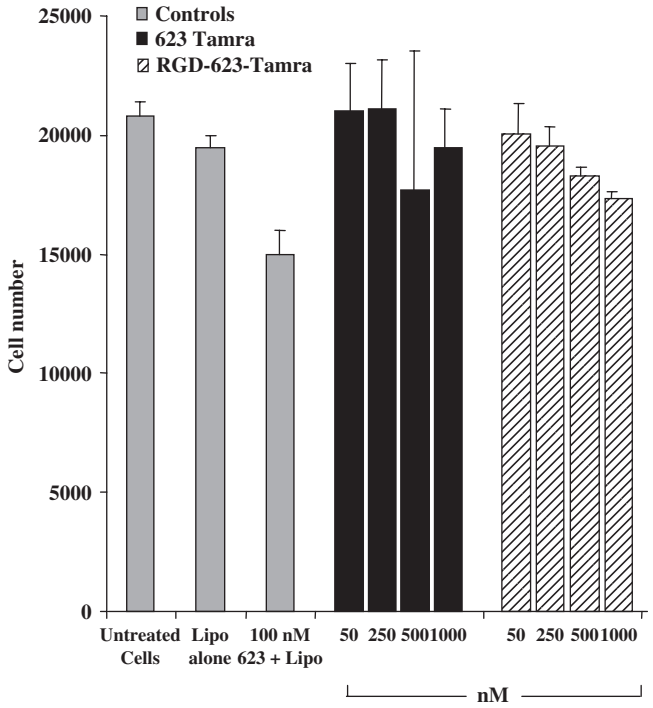

Figure 8. Short-term toxicity of 623–RGD conjugates. Cells were treated with either 623-Tamra, 623-Tamra complexed with Lipofectamine 2000 or RGD–623-Tamra conjugate, as described in Materials and methods section, and viable cell numbers were determined after 48 h by using a particle counter. Gray bars represent cell numbers of various controls i.e. cells treated with Lipofectamine 2000 (Lipo), and 623-Tamra complexed with Lipofectamine 2000. Black bars represent cell numbers for 623-Tamra, and patterned/striped bars represent RGD–623-Tamra conjugate, all at the indicated concentrations. Results are means and standard errors of three determinations.

The mechanism(s) by which receptor-mediated endocytosis enhances the activity of anionic antisense and siRNA oligonucleotides is unclear. Obviously one aspect is the increased intracellular uptake of the ligand–oligonucleotide conjugate compared to free oligonucleotide. However, this cannot be the only factor involved, since we and others have found that increased accumulation of anionic oligonucleotides caused by conjugation or complexation with polycationic peptides or polymers does not necessarily result in biologically effective delivery (21,22,39,69). In the cases of cationic lipids, or polymers with secondary amines such as PEI, their efficacy as nucleic acid carriers seems to be due to endosome-disrupting effects, thus allowing release of the active material into the cytosol (70); however, such endosome-damaging effects are unlikely when using RGD peptides as carriers.

An alternative mechanism may involve the particular intracellular trafficking pathway of the RGD–oligonucleotide conjugates as they are initially transported by integrins. There are several distinct mechanisms of endocytosis, each leading to endosomal trafficking patterns that have unique as well as overlapping features (42). Integrins are known to recycle via internalization into endosomal compartments (71), but the exact pathways and mechanisms involved are not fully resolved. Some studies indicate that the αvβ3 integrin is normally internalized via caveolae and then takes the so-called 'long loop' Rab 11-dependent recycling pathway back to the plasma membrane through the perinuclear recycling compartment (71,72). Our studies of the trafficking of the RGD-conjugate suggest that initial uptake involves caveolae and possibly other smooth, non-clathrin-coated vesicles and that some of the conjugate is eventually delivered to the trans-Golgi. Thus, the initial phase of uptake seems consistent with the path described for the αvβ3 integrin, but later phases seem distinct. This is not surprising since ligands and their receptors often diverge during intracellular trafficking. In an interesting parallel, recent studies have suggested that trafficking through the Golgi is also a productive route for functional delivery of siRNA (53,73).

We have noticed that conjugation of the RGD moiety results in only a 2- to 3-fold increase in cell uptake versus the unconjugated 623 oligonucleotide, but a several-fold

Table 2. Lack of long-term toxicity of RGD–oligonucleotide conjugates

Material tested in soft agar assay	Lipofectamine 2000 Control	Lipofectamine + 100 nM 623 Tamra	50 nM 623-Tamra	500 nM 623-Tamra	50 nM RGD–623-Tamra	250 nM RGD–623-Tamra	1000 nM RGD–623-Tamra
Colonies formed/100 cells plated	13.3 ± 3.0	13.8 ± 2.0	14.8 ± 3.0	13.0 ± 2.5	15.3 ± 2.5	13.7 ± 1.2	14.0 ± 2.0

A373SM-Luc 705B melanoma cells were treated with the indicated materials under the same conditions as those used for the luciferase induction assays. Thereafter, cells were harvested, diluted and suspended in soft agar in 6-well plates with complete growth medium. Plates were incubated for 14 days and colonies >25 cells were counted. Results are shown as colonies per 100 cells plated and are the means and SDs of at least 6 wells per treatment. Note: colony formation by untreated melanoma cells was not different from that of the Lipofectamine 2000 control.

increase in biological effect. This hints that the initial uptake pathway may affect the ultimate delivery event; however, for the present this remains an untested hypothesis. Confirmation will require a much more detailed analysis of the subcellular trafficking pattern of this and other conjugates in relation to their biological effects. In any case, the apparent effectiveness of the RGD–oligonucleotide conjugates in attaining splice correction suggests that their mechanism of action will warrant further investigation both in cell culture and in the *in vivo* context.

SUPPLEMENTARY DATA

Supplementary Data are available at NAR Online.

ACKNOWLEDGEMENTS

The authors wish to thank Betsy Clarke for expert editorial assistance and Priscila Siesser for assistance with flow cytometry. This study was supported by NIH grant PO1 GM59299 to R.L.J and by grants from the National Cancer Institute (R21 CA121842, P50 CA114747, U54CA119367) and Department of Defense (W81XWH-07-1-0374) to X.C. Funding to pay the Open Access publication charges for this article was provided by PO1 GM59299.

Conflict of interest statement. None declared.

REFERENCES

1. Kurreck,J. (2003) Antisense technologies. Improvement through novel chemical modifications. *Eur. J. Biochem.*, **270**, 1628–1644.
2. Manoharan,M. (2002) Oligonucleotide conjugates as potential antisense drugs with improved uptake, biodistribution, targeted delivery, and mechanism of action. *Antisense Nucleic Acid Drug Dev.*, **12**, 103–128.
3. Fisher,M., Abramov,M., Van Aerschot,A., Xu,D., Juliano,R.L. and Herdewijn,P. (2007) Inhibition of MDR1 expression with altritol-modified siRNAs. *Nucleic Acids Res.*, **35**, 1064–1074.
4. Juliano,R.L. and Yoo,H. (2000) Aspects of the transport and delivery of antisense oligonucleotides. *Curr. Opin. Mol. Ther.*, **2**, 297–303.
5. Inoue,A., Sawata,S.Y. and Taira,K. (2006) Molecular design and delivery of siRNA. *J. Drug. Target.*, **14**, 448–455.
6. Crooke,S.T. (2004) Progress in antisense technology. *Annu. Rev. Med.*, **55**, 61–95.
7. Soutschek,J., Akinc,A., Bramlage,B., Charisse,K., Constien,R., Donoghue,M., Elbashir,S., Geick,A., Hadwiger,P., Harborth,J. *et al.* (2004) Therapeutic silencing of an endogenous gene by systemic administration of modified siRNAs. *Nature*, **432**, 173–178.
8. Kim,D.H. and Rossi,J.J. (2007) Strategies for silencing human disease using RNA interference. *Nat. Rev. Genet.*, **8**, 173–184.
9. Coppelli,F.M. and Grandis,J.R. (2005) Oligonucleotides as anticancer agents: from the benchside to the clinic and beyond. *Curr. Pharm. Des.*, **11**, 2825–2840.
10. Van den Haute,C., Eggermont,K., Nuttin,B., Debyser,Z. and Baekelandt,V. (2003) Lentiviral vector-mediated delivery of short hairpin RNA results in persistent knockdown of gene expression in mouse brain. *Hum. Gene. Ther.*, **14**, 1799–1807.
11. McCaffrey,A.P., Meuse,L., Pham,T.T., Conklin,D.S., Hannon,G.J. and Kay,M.A. (2002) RNA interference in adult mice. *Nature*, **418**, 38–39.
12. Xu,D., McCarty,D., Fernandes,A., Fisher,M., Samulski,R.J. and Juliano,R.L. (2005) Delivery of MDR1 small interfering RNA by self-complementary recombinant adeno-associated virus vector. *Mol. Ther.*, **11**, 523–530.
13. Hu-Lieskovan,S., Heidel,J.D., Bartlett,D.W., Davis,M.E. and Triche,T.J. (2005) Sequence-specific knockdown of EWS-FLI1 by targeted, nonviral delivery of small interfering RNA inhibits tumor growth in a murine model of metastatic Ewing's sarcoma. *Cancer Res.*, **65**, 8984–8992.
14. Oishi,M., Hayama,T., Akiyama,Y., Takae,S., Harada,A., Yamasaki,Y., Nagatsugi,F., Sasaki,S., Nagasaki,Y. and Kataoka,K. (2005) Supramolecular assemblies for the cytoplasmic delivery of antisense oligodeoxynucleotide: polyion complex (PIC) micelles based on poly(ethylene glycol)-SS-oligodeoxynucleotide conjugate. *Biomacromolecules*, **6**, 2449–2454.
15. Vinogradov,S.V., Batrakova,E.V. and Kabanov,A.V. (2004) Nanogels for oligonucleotide delivery to the brain. *Bioconjugate Chem.*, **15**, 50–60.
16. Fattal,E., Couvreur,P. and Dubernet,C. (2004) "Smart" delivery of antisense oligonucleotides by anionic pH-sensitive liposomes. *Adv Drug Deliv Rev*, **56**, 931–946.
17. Yoo,H. and Juliano,R.L. (2000) Enhanced delivery of antisense oligonucleotides with fluorophore-conjugated PAMAM dendrimers. *Nucleic Acids Res.*, **28**, 4225–4231.
18. Juliano,R.L. (2007) Biological Barriers to Nanocarrier-Mediated Delivery of Therapeutic and Imaging Agents. In Mirkin,C. and Niemeyer,C. (eds.), *Nanobiotechnology*. Vol. 2, Wiley and Sons, New York, pp. 263–84.
19. Jarver,P. and Langel,U. (2004) The use of cell-penetrating peptides as a tool for gene regulation. *Drug Discov. Today*, **9**, 395–402.
20. Wadia,J.S. and Dowdy,S.F. (2002) Protein transduction technology. *Curr. Opin. Biotechnol.*, **13**, 52–56.
21. Juliano,R.L. (2005) Peptide-oligonucleotide conjugates for the delivery of antisense and siRNA. *Curr. Opin. Mol. Ther.*, **7**, 132–136.
22. Abes,S., Moulton,H., Turner,J., Clair,P., Richard,J.P., Iversen,P., Gait,M.J. and Lebleu,B. (2007) Peptide-based delivery of nucleic acids: design, mechanism of uptake and applications to splice-correcting oligonucleotides. *Biochem. Soc. Trans.*, **35**, 53–55.
23. Astriab-Fisher,A., Sergueev,D., Fisher,M., Shaw,B.R. and Juliano,R.L. (2002) Conjugates of antisense oligonucleotides with the Tat and antennapedia cell-penetrating peptides: effects on cellular uptake, binding to target sequences, and biologic actions. *Pharm. Res.*, **19**, 744–754.
24. Astriab-Fisher,A., Sergueev,D.S., Fisher,M., Shaw,B.R. and Juliano,R.L. (2000) Antisense inhibition of P-glycoprotein expression using peptide-oligonucleotide conjugates. *Biochem. Pharmacol.*, **60**, 83–90.
25. Muratovska,A. and Eccles,M.R. (2004) Conjugate for efficient delivery of short interfering RNA (siRNA) into mammalian cells. *FEBS Lett.*, **558**, 63–68.
26. Chiu,Y.L., Ali,A., Chu,C.Y., Cao,H. and Rana,T.M. (2004) Visualizing a correlation between siRNA localization, cellular uptake, and RNAi in living cells. *Chem. Biol.*, **11**, 1165–1175.
27. Turner,J.J., Ivanova,G.D., Verbeure,B., Williams,D., Arzumanov,A.A., Abes,S., Lebleu,B. and Gait,M.J. (2005) Cell-penetrating peptide conjugates of peptide nucleic acids (PNA) as inhibitors of HIV-1 Tat-dependent trans-activation in cells. *Nucleic Acids Res.*, **33**, 6837–6849.
28. El-Andaloussi,S., Johansson,H.J., Lundberg,P. and Langel,U. (2006) Induction of splice correction by cell-penetrating peptide nucleic acids. *J. Gene. Med.*, **8**, 1262–1273.
29. Bendifallah,N., Rasmussen,F.W., Zachar,V., Ebbesen,P., Nielsen,P.E. and Koppelhus,U. (2006) Evaluation of cell-penetrating peptides (CPPs) as vehicles for intracellular delivery of antisense peptide nucleic acid (PNA). *Bioconjugate Chem.*, **17**, 750–758.
30. Moulton,H.M., Hase,M.C., Smith,K.M. and Iversen,P.L. (2003) HIV Tat peptide enhances cellular delivery of antisense morpholino oligomers. *Antisense Nucleic Acid Drug. Dev.*, **13**, 31–43.
31. Abes,S., Turner,J.J., Ivanova,G.D., Owen,D., Williams,D., Arzumanov,A., Clair,P., Gait,M.J. and Lebleu,B. (2007) Efficient splicing correction by PNA conjugation to an R6-Penetratin delivery peptide. *Nucleic Acids Res.*, **35**, 4495–4502.
32. McNamara,J.O.,2nd, Andrechek,E.R., Wang,Y., Viles,K.D., Rempel,R.E., Gilboa,E., Sullenger,B.A. and Giangrande,P.H. (2006) Cell type-specific delivery of siRNAs with aptamer-siRNA chimeras. *Nat. Biotechnol.*, **24**, 1005–1015.

33. Song,E., Zhu,P., Lee,S.K., Chowdhury,D., Kussman,S., Dykxhoorn,D.M., Feng,Y., Palliser,D., Weiner,D.B., Shankar,P. *et al.* (2005) Antibody mediated in vivo delivery of small interfering RNAs via cell-surface receptors. *Nat. Biotechnol.*, **23**, 709–717.
34. Tian,X., Aruva,M.R., Qin,W., Zhu,W., Sauter,E.R., Thakur,M.L. and Wickstrom,E. (2005) Noninvasive molecular imaging of MYC mRNA expression in human breast cancer xenografts with a [99mTc]peptide-peptide nucleic acid-peptide chimera. *Bioconjugate Chem.*, **16**, 70–79.
35. Chen,X., Plasencia,C., Hou,Y. and Neamati,N. (2005) Synthesis and biological evaluation of dimeric RGD peptide-paclitaxel conjugate as a model for integrin-targeted drug delivery. *J. Med. Chem.*, **48**, 1098–1106.
36. Juliano,R.L. (2002) Signal transduction by cell adhesion receptors and the cytoskeleton: functions of integrins, cadherins, selectins, and immunoglobulin-superfamily members. *Annu. Rev. Pharmacol Toxicol.*, **42**, 283–323.
37. Stupack,D.G. and Cheresh,D.A. (2004) Integrins and angiogenesis. *Curr. Top. Dev. Biol.*, **64**, 207–238.
38. Kang,S.H., Cho,M.J. and Kole,R. (1998) Up-regulation of luciferase gene expression with antisense oligonucleotides: implications and applications in functional assay development. *Biochemistry*, **37**, 6235–6239.
39. Turner,J.J., Arzumanov,A.A. and Gait,M.J. (2005) Synthesis, cellular uptake and HIV-1 Tat-dependent trans-activation inhibition activity of oligonucleotide analogues disulphide-conjugated to cell-penetrating peptides. *Nucleic Acids Res.*, **33**, 27–42.
40. Felding-Habermann,B., Mueller,B.M., Romerdahl,C.A. and Cheresh,D.A. (1992) Involvement of integrin alpha V gene expression in human melanoma tumorigenicity. *J. Clin. Invest.*, **89**, 2018–2022.
41. Astriab-Fisher,A., Fisher,M.H., Juliano,R. and Herdewijn,P. (2004) Increased uptake of antisense oligonucleotides by delivery as double stranded complexes. *Biochem. Pharmacol.*, **68**, 403–407.
42. Perret,E., Lakkaraju,A., Deborde,S., Schreiner,R. and Rodriguez-Boulan,E. (2005) Evolving endosomes: how many varieties and why? *Curr. Opin. Cell Biol.*, **17**, 423–434.
43. Butler,M., Stecker,K. and Bennett,C.F. (1997) Cellular distribution of phosphorothioate oligodeoxynucleotides in normal rodent tissues. *Lab. Invest.*, **77**, 379–388.
44. Babuke,T. and Tikkanen,R. (2007) Dissecting the molecular function of reggie/flotillin proteins. *Eur. J. Cell Biol.*, **86**, 525–532.
45. Zerial,M. and McBride,H. (2001) Rab proteins as membrane organizers. *Nat. Rev. Mol. Cell Biol.*, **2**, 107–117.
46. Gullapalli,A., Wolfe,B.L., Griffin,C.T., Magnuson,T. and Trejo,J. (2006) An essential role for SNX1 in lysosomal sorting of protease-activated receptor-1: evidence for retromer-, Hrs-, and Tsg101-independent functions of sorting nexins. *Mol. Biol. Cell*, **17**, 1228–1238.
47. Wolfe,B.L., Marchese,A. and Trejo,J. (2007) Ubiquitination differentially regulates clathrin-dependent internalization of protease-activated receptor-1. *J. Cell Biol.*, **177**, 905–916.
48. Kole,R., Vacek,M. and Williams,T. (2004) Modification of alternative splicing by antisense therapeutics. *Oligonucleotides*, **14**, 65–74.
49. Resina,S., Kole,R., Travo,A., Lebleu,B. and Thierry,A.R. (2007) Switching on transgene expression by correcting aberrant splicing using multi-targeting steric-blocking oligonucleotides. *J. Gene. Med.*, **9**, 498–510.
50. Friedlander,M., Theesfeld,C.L., Sugita,M., Fruttiger,M., Thomas,M.A., Chang,S. and Cheresh,D.A. (1996) Involvement of integrins alpha v beta 3 and alpha v beta 5 in ocular neovascular diseases. *Proc. Natl Acad. Sci. USA*, **93**, 9764–9769.
51. Mitra,A., Coleman,T., Borgman,M., Nan,A., Ghandehari,H. and Line,B.R. (2006) Polymeric conjugates of mono- and bi-cyclic alphaVbeta3 binding peptides for tumor targeting. *J. Control Rel.*, **114**, 175–183.
52. Kirkham,M. and Parton,R.G. (2005) Clathrin-independent endocytosis: new insights into caveolae and non-caveolar lipid raft carriers. *Biochim. Biophys. Acta.*, **1745**, 273–286.
53. Overhoff,M. and Sczakiel,G. (2005) Phosphorothioate-stimulated uptake of short interfering RNA by human cells. *EMBO Rep.*, **6**, 1176–1181.
54. Parpal,S., Karlsson,M., Thorn,H. and Stralfors,P. (2001) Cholesterol depletion disrupts caveolae and insulin receptor signaling for metabolic control via insulin receptor substrate-1, but not for mitogen-activated protein kinase control. *J. Biol. Chem.*, **276**, 9670–9678.
55. Aplin,A.E. and Juliano,R.L. (1999) Integrin and cytoskeletal regulation of growth factor signaling to the MAP kinase pathway. *J. Cell Sci.*, **112(Pt 5),** 695–706.
56. Lv,H., Zhang,S., Wang,B., Cui,S. and Yan,J. (2006) Toxicity of cationic lipids and cationic polymers in gene delivery. *J. Control Rel.*, **114**, 100–109.
57. Smith,C.W. and Valcarcel,J. (2000) Alternative pre-mRNA splicing: the logic of combinatorial control. *Trends Biochem. Sci.*, **25**, 381–388.
58. Villien,M., Defrancq,E. and Dumy,P. (2004) Chemoselective oxime and thiazolidine bond formation: a versatile and efficient route to the preparation of 3'-peptide-oligonucleotide conjugates. *Nucleos. Nucleot. Nucl.*, **23**, 1657–1666.
59. Harrison,J.G. and Balasubramanian,S. (1998) Synthesis and hybridization analysis of a small library of peptide-oligonucleotide conjugates. *Nucleic Acids Res.*, **26**, 3136–3145.
60. Mier,W., Eritja,R., Mohammed,A., Haberkorn,U. and Eisenhut,M. (2000) Preparation and evaluation of tumor-targeting peptide-oligonucleotide conjugates. *Bioconjugate Chem.*, **11**, 855–860.
61. Zatsepin,T.S., Stetsenko,D.A., Arzumanov,A.A., Romanova,E.A., Gait,M.J. and Oretskaya,T.S. (2002) Synthesis of peptide-oligonucleotide conjugates with single and multiple peptides attached to 2'-aldehydes through thiazolidine, oxime, and hydrazine linkages. *Bioconjugate Chem.*, **13**, 822–830.
62. Dijkgraaf,I., Liu,S., Kruijtzer,J.A., Soede,A.C., Oyen,W.J., Liskamp,R.M., Corstens,F.H. and Boerman,O.C. (2007) Effects of linker variation on the in vitro and in vivo characteristics of an 111In-labeled RGD peptide. *Nucl. Med. Biol.*, **34**, 29–35.
63. Li,Z.B., Cai,W., Cao,Q., Chen,K., Wu,Z., He,L. and Chen,X. (2007) 64Cu-labeled tetrameric and octameric RGD peptides for small-animal PET of tumor {alpha}v{beta}3 integrin expression. *J. Nucl. Med.*, **48**, 1162–1171.
64. Chen,X. (2006) Multimodality imaging of tumor integrin alphavbeta3 expression. *Mini Rev. Med. Chem.*, **6**, 227–234.
65. Temming,K., Lacombe,M., van der Hoeven,P., Prakash,J., Gonzalo,T., Dijkers,E.C., Orfi,L., Keri,G., Poelstra,K., Molema,G. *et al.* (2006) Delivery of the p38 MAPkinase inhibitor SB202190 to angiogenic endothelial cells: development of novel RGD-equipped and PEGylated drug-albumin conjugates using platinum(II)-based drug linker technology. *Bioconjugate Chem.*, **17**, 1246–1255.
66. Cai,W., Shin,D.W., Chen,K., Gheysens,O., Cao,Q., Wang,S.X., Gambhir,S.S. and Chen,X. (2006) Peptide-labeled near-infrared quantum dots for imaging tumor vasculature in living subjects. *Nano Lett.*, **6**, 669–676.
67. Ikeda,Y. and Taira,K. (2006) Ligand-targeted delivery of therapeutic siRNA. *Pharm Res.*, **23**, 1631–1640.
68. Hwa Kim,S., Hoon Jeong,J., Chul Cho,K., Wan Kim,S. and Gwan Park,T. (2005) Target-specific gene silencing by siRNA plasmid DNA complexed with folate-modified poly(ethylenimine). *J. Control Rel.*, **104**, 223–232.
69. Lundberg,P., El-Andaloussi,S., Sutlu,T., Johansson,H. and Langel,U. (2007) Delivery of short interfering RNA using endosomolytic cell-penetrating peptides. *FASEB J.*, **21**, 2664–2671.
70. Hoekstra,D., Rejman,J., Wasungu,L., Shi,F. and Zuhorn,I. (2007) Gene delivery by cationic lipids: in and out of an endosome. *Biochem. Soc. Trans.*, **35**, 68–71.
71. Caswell,P.T. and Norman,J.C. (2006) Integrin trafficking and the control of cell migration. *Traffic*, **7**, 14–21.
72. White,D.P., Caswell,P.T. and Norman,J.C. (2007) alpha v beta3 and alpha5beta1 integrin recycling pathways dictate downstream Rho kinase signaling to regulate persistent cell migration. *J. Cell Biol.*, **177**, 515–525.
73. Mescalchin,A., Detzer,A., Wecke,M., Overhoff,M., Wunsche,W. and Sczakiel,G. (2007) Cellular uptake and intracellular release are major obstacles to the therapeutic application of siRNA: novel options by phosphorothioate-stimulated delivery. *Expert Opin. Biol. Th.*, **7**, 1531–1538.